Current spreading length and injection efficiency in ZnO/GaN-based light-emitting diodes

Roberto Macaluso, Giuseppe Lullo, Isodiana Crupi, Fulvio Caruso, Eric Feltin, Mauro Mosca

***Abstract*—We report on carrier injection features in light-emitting diodes (LEDs) based on *non-intentionally doped*-ZnO/*p*-GaN heterostructures. These LEDs consist of a ZnO layer grown by chemical bath deposition (CBD) onto a *p*-GaN template without using any seed layer. The ZnO layer (~1 μm thickness) consists of a dense collection of partially-coalesced ZnO nanorods, organized in wurtzite phase with marked vertical orientation, whose density depends on the concentration of the solution during the CBD process. Due to the limited conductivity of the *p*-GaN layer, the recombination in the *n*-region is strongly dependent on the spreading length of the holes, L_h, coming from the *p*-contact. Moreover, the evaluation of L_h is not easy and generally requires the design and the fabrication of several LED test-patterns. We propose a simple and effective method to calculate L_h, just based on simple considerations on *I-V* characteristics, and a way to improve the injection efficiency in the *n* region based on a non-circular electrode geometry. In particular, an interdigitated electrode structure is proved to be more efficient in terms of hole injection from *n*- to *p*- region.**

***Index Terms*—ZnO/GaN heterostructures, ZnO/GaN-based light-emitting diodes, current spreading length, contact injection, chemical bath deposition of ZnO nanorods**

I. INTRODUCTION

Zinc oxide (ZnO) is an *n*-type semiconductor material, easy to grow in a nanostructured form [1], with a wide direct bandgap (3.37 eV), a high exciton binding energy (60 meV) at room temperature, and exciting optoelectronic properties [2]. In particular, the larger exciton binding energy, compared to that of GaN (24 meV), would allow the realization of high-efficiency light-emitting diodes (LEDs) and lasers working at room temperature. Due to these excellent properties, ZnO is regarded as a promising candidate for the fabrication of ultraviolet [3]–[6], blue [4], [7]–[9], white LEDs, with and without any phosphor or dye [10]–[13]. Nevertheless, ZnO homojunction LEDs never made a significant breakthrough because of the difficulties in fabricating reproducible and stable *p*-type ZnO, due to low solubility of acceptor dopants, self-compensating effects, and height of acceptor's level energy. Although many research groups have reported on ZnO-based homostructure LEDs, the results are controversial as reviewed in [14].

The wurtzite hexagonal structure, the small in-plane lattice mismatch with ZnO (1.8%), and the minor band offset with ZnO allowed doped and undoped GaN to be widely used in various fields, together with ZnO [15]–[19], and in particular, to make heterojunction LEDs based on an *n*-ZnO/*p*-GaN structure. Unfortunately, the radiative recombination in such LEDs occurs mainly in the *p*-GaN side, since the electrons injected from ZnO to GaN are dominating the light emission process. In fact, due to the higher doping concentration of ZnO (generally higher than GaN), the depletion region primarily extends to the *p*-GaN semiconductor. Other reasons, described by Rogers *et al.* in [6], are i) the band line-up which makes the electron injection from the ZnO more energetically favorable than the hole injection from the *p*-GaN, and ii) the low quality epitaxy of ZnO which is responsible of a large defect/dislocation density at the ZnO/GaN interface. Consequently, it is not easy to exploit the optoelectronic properties of ZnO, in particular its high exciton binding energy.

Devices based on *n*-ZnO/*p*-GaN heterojunctions could also benefit from strong excitonic emission if the radiative recombination occurred in the ZnO layer; nevertheless, for the abovementioned reasons, plenty of works report radiative recombination occurring primarily in the GaN side of the junction [7], [9], [20], [21].

The quality of a *n*-ZnO/*p*-GaN heterojunction mainly depends on the method used to grow the ZnO film on GaN [20], [22]–[24]. Generally, the poor quality of the interface produces low emission efficiencies. Furthermore, *n*-ZnO/*p*-GaN heterojunction LEDs suffer from high reverse leakage current and large turn-on voltage, due to the porous nature of the ZnO layer [25].

In order to promote the growth of ZnO on *p*-GaN in the form of nanorod, nanotube, or simple film, a ZnO seed layer previously deposited on *p*-GaN is generally used, especially if a re-growth is performed by chemical bath deposition techniques. A seed layer is often necessary to achieve the self-alignment or the vertical orientation of re-grown nanostructures. However, the seed layer, whose thickness is usually a few tens of nm, behaves as an interface layer which affects the light emission and extraction and may introduce

(Corresponding author: Mauro Mosca.)

R. Macaluso, G. Lullo, I. Crupi, and M. Mosca are with the Department of Engineering, University of Palermo, Viale delle Scienze, Building 9, I-90128 Palermo, Italy (e-mail: roberto.macaluso@unipa.it, giuseppe.lullo@unipa.it, isodiana.crupi@unipa.it, mauro.mosca@unipa.it).

F. Caruso was with the Department of Engineering, University of Palermo, Viale delle Scienze, Building 9, I-90128 Palermo, Italy. He is now with ABB Asea Brown Boveri Ltd., Affolternstrasse 44, CH-8050 Zurich, Switzerland.

Eric Feltin is with Novagan Sàrl, EPFL Innovation Park, Building D, CH-1015 Lausanne, Switzerland (e-mail: eric.feltin@novagan.com).

interfacial defects [4], [8]. The effective utility of the seed layer is a controversial matter, and can be subject of a scientific debate on its own. Actually, a few authors reported on vertically-aligned ZnO nanorods on *p*-GaN, with good optical and structural properties, grown without a seed layer [26]–[28].

Apart from the aforementioned limitations, radiative efficiency in a *n*-ZnO/*p*-GaN heterojunction based-LED is severely affected by limited carrier transport in the *p*-GaN layer, due to both its poor electrical conductivity and its high contact resistance. In a standard GaN based-homojunction LED, the *p*-layer is grown onto the *n*-layer, whose electrical conductivity is several orders of magnitude larger than that of the *p*-layer; consequently, in a lateral LED based on a mesa structure (Fig. 1.a) the recombination occurs in correspondence of the *p*-contact and the emission intensity is almost independent of the position of the *n*-contacts. On the contrary, in an *n*-ZnO/*p*-GaN based-heterojunction LED the base layer is the *p*-type GaN while the *n*-type ZnO is re-grown above of it.

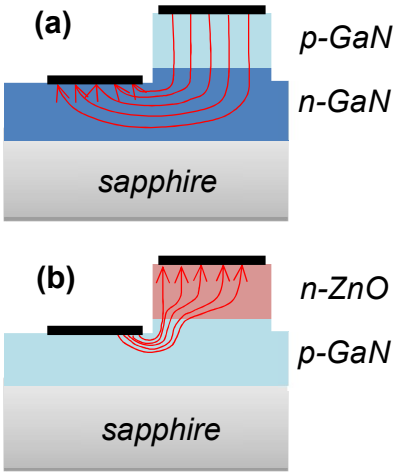

Fig. 1. (a) Current lines in a typical GaN-based homojunction LED and (b) in a *n*-ZnO/*p*-GaN based-heterojunction LED.

A typical layout consists of a bottom, annular-shaped, metal contact on *p*-GaN, surrounding a thin film of ZnO with a circular pad above. In this case, both the radiative efficiency and the *I-V* characteristic of the device strongly depend on the conductivity of the *p*-GaN layer. In fact, in order to have a uniform emission, the holes injected from the annular *p*-contact should travel through the *p*-GaN for a maximum distance equal to the radius of the circular pad covering the *n*-ZnO. If the device has a very large radius, the holes may not spread for the full length of the *n*-pad (Fig. 1.b). As a consequence, the active area where the radiative recombination takes place is small and confined to the perimeter of the *n*-contact. Light emission is annular and non-uniform through the device, this phenomenon having a greater incidence as the device size increases. This could hinder a large-scale mass production given that commercial LEDs are typically 1 mm × 1 mm sized. Surprisingly, very few researchers mentioned this problem in their studies, and even less discussed about it.

Both the limited carrier transport in the *p*-GaN layer, and the complexity of the evaluation of current spreading length motivate the research of a simple and practical method to find the spreading length of the hole current coming from the *p*- to the *n*-contact of the heterojunction LEDs. In fact, unfortunately most of the models used to calculate the current spreading length are based on works of Guo and Schubert [29], [30], which require the knowledge of an abundant number of parameters and the implementation of a special contact pattern onto the wafer surface. Moreover, all the calculations were made only for GaN-based homojunctions LEDs and no results are available for ZnO/GaN-based heterojunction LEDs.

In this work we report on the fabrication and the characterization of non-intentionally doped *nid*-ZnO/*p*-GaN heterojunction-based LEDs with different electrode sizes and shapes, and different distances between *n*- and *p*-contacts. As-grown, *nid*-ZnO films show native *n*-type doping. This is nowadays attributed to a molecular complex consisting of an oxygen vacancy and a hydrogen atom, which behaves as a shallow donor (0.8 eV) [31].

ZnO was deposited on *p*-GaN templates by chemical-bath deposition (CBD), which is a simple and inexpensive technique used to grow ZnO nanostructures [32]. The correlation between carrier transport and *I-V* characteristics was evidenced and a simple and practical method to evaluate the spreading length of the hole current was proposed. Furthermore, the use of interdigitated shape contacts as a way to improve charge transport efficiency was introduced and tested.

II. Experimental Details

The template used for LED fabrication consists of a (*p*-*n*)GaN structure, with 100 nm of *p*-GaN, grown on a 1 µm-thick *n*-GaN on a *c*-plane 2-inch sapphire wafer. GaN was grown by metal-organic vapor-phase epitaxy (MOVPE) on a 2-inch *c*-plane sapphire substrate in an AIXTRON 200/4 RF-S reactor, using triethylgallium (TEGa), ammonia (NH_3) and bis (cyclopentadienyl) magnesium (Cp_2Mg) as the metal–organic precursors for Ga, N and Mg, respectively. Subsequently, the wafer was cut into small chips of approximately 1 cm^2 before being processed with direct laser writing lithography for both ZnO area definition and metal contacts patterning. First, bottom metal electrodes (100 nm-thick Cu contacts) were patterned and deposited by thermal evaporation onto the *p*-GaN layer, then a second photolithography step was performed to define the regions where growing the ZnO coalesced nanorods; finally, after ZnO growth, Al contacts (100 nm) were deposited onto the ZnO regions. ZnO nanorods preparation by CBD has been widely described in a previous work [26]. After definition of the areas intended to be covered by ZnO, samples were immersed in a 50 mM-concentrated nutrient solution, prepared with zinc nitrate hexahydrate (Sigma-Aldrich, reagent grade 98%) and hexamethylenetetramine (Alfa Aesar, ACS 99+%) in deionized water, while being heated at a temperature of 80 °C for 3 hours. Then, the samples were left in the solution to cool naturally at room temperature. Afterwards, the samples were rinsed with distilled water and then with acetone and isopropanol.

Structural properties of the ZnO layers were estimated by x-ray diffraction (XRD) with Cu K-α radiation (λ = 1.5405980 Å), a generator voltage of 40 kV and a tube current of 30 mA. Optical properties were evaluated by photoluminescence measurements by using the third harmonic of a Nd:YAG laser (355 nm). To measure the optical and electrical performances of the devices a light power-current-voltage (L-I-V) setup was used. The electroluminescence of the LEDs was measured by an Ocean Optics HR4000CG UV-VIS spectrometer.

III. Results and Discussion

A. ZnO nanorods

The *nid*-ZnO layer (~1 µm thickness), consisting of a dense collection of partially-coalesced ZnO nanorods, appears as shown in the scanning-electron microscope (SEM) image of Fig. 2. The coalescence process of the nanorods is large with highly-concentrated solutions [33], [34]. A dense nanorods layer is less fragile and allows easier handling during the subsequent metal contacts fabrication

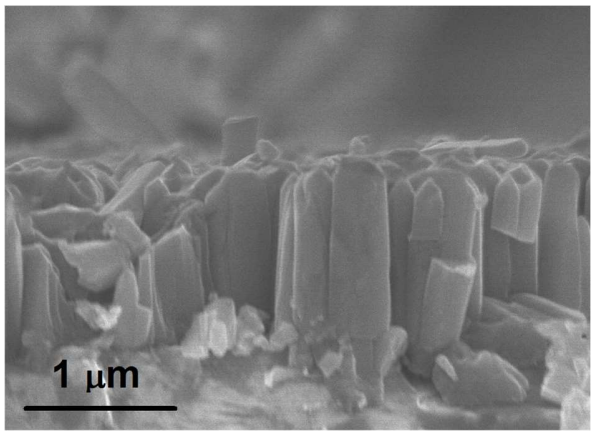

Fig. 2. Cross section SEM image of ZnO nanorods grown by chemical bath deposition (3 hours, 50 mM-concentrated nutrient solution).

XRD analysis shows two strong diffraction peaks, located at 34.43° and 72.74°, in good agreement with those reported for ZnO (002) and ZnO (004), respectively, in JCPDS # 36-1451, confirming that the CBD technique leads to wurtzite nanostructures with marked vertical orientation. Other details on XRD analysis are reported in [26].

B. Effects of distances between contacts

Fig. 3 shows the electrical characteristics *I-V* of circular-shaped LEDs with a diameter of 200 µm as a function of distance *d* between the ZnO region and the *p* electrode (either 5 or 20 µm). A sketch of the LED structure, together with an optical microscope image of the processed LED, are reported in the inset of the same figure. The LEDs have a dominant violet emission at 395 nm, corresponding to the photoluminescence peak of ZnO.

The *I-V* characteristics demonstrate that the injected current (for a fixed voltage) decreases as the distance between the electrodes increases, since the hole transport is limited by the

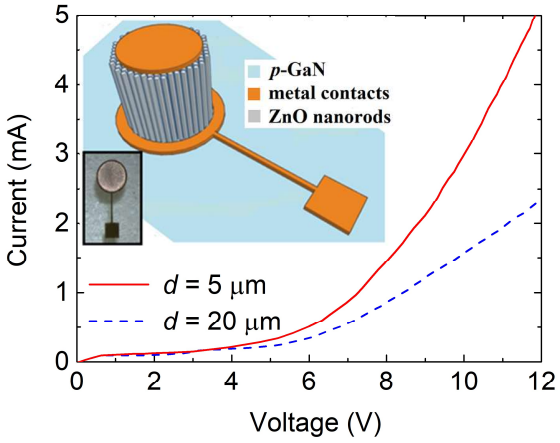

Fig. 3. *I-V* characteristics of 200 µm-LEDs for different distances between the *n*- and the *p*-contact. Inset: Sketch of the LED structure and optical microscope image of the processed device.

poor conductivity of *p*-GaN. Moreover, the holes can recombine with the injected electrons only at small distances from the annular *p*-contact. So, the light emission is not uniform and the photons are emitted only near to the edge of the circular contact, even if the spatial gap between the contacts is small. This is more evident for LEDs with great *n*-contact surface, where the distance to be covered by the holes is relatively large. With regards to the negative bias region of the *I-V* characteristics it is worth to point out that current losses are quite high (several milliamperes at -5 V), due to the porous structure with partial or non-coalesced nanorods which induces conductive micro-channels between *n*- and *p*-regions.

C. Current spreading in large-surface LEDs

In order to have a homogeneous emission from a *nid*-ZnO/*p*-GaN heterojunction-based LED, the holes should be uniformly injected from the bottom *p*-GaN layer into the ZnO top layer. Lateral injection of the holes is limited by the spreading length of the hole current. The emission is uniform if the hole current spreading length, L_h, is at least equal to the *n*-contact radius plus the distance between *n*- and *p*-contacts, so that the holes coming from the *p*-contact can be effectively injected to the center of the *n*-contact. Clearly, in large-surface *n*-contacts, the center of the *n*-contact is too distant from the *p*-contact and the recombination mainly occurs in the region around the border of the *n*-contact. The picture in the inset of Fig. 4(a) shows the non-uniformity of the recombination in such an LED at low injection regime: light is mainly emitted from the border of the *n*- contact.

The method to calculate the hole current spreading length is based on a simple assertion: if the hole injection is perfectly uniform under the whole *n*-contact ($L_h \rightarrow \infty$), the current density *J* measured at a fixed voltage in LEDs with different *n*-contact sizes is always the same. Fig. 4(a) shows *I-V* characteristics for two LEDs, respectively sized 200 and 500 µm (diameter of *n*-contact), with a *n-p* contact interspace of 20

μm. The current density J is calculated dividing the flowing current by the whole area of the n-contact, equal to 3.14×10^{-4} cm^2 for the 200 μm-diameter and 1.96×10^{-3} cm^2 for the 500 μm-diameter. The corresponding J-V characteristics are shown in Fig. 4(b). The two curves are not coincident because the spreading area is different from the n-contact area. Supposing, as actually is, the spreading area is smaller than the n-contact surface, the curves can be superimposed if one considers as current density the ratio between the measured current and the real spreading area. The latter is an annulus whose area A^* is calculated as:

$$A^* = \pi[r_c^2 - (r_c - L_h)^2] \quad (1)$$

where r_c is the radius of the circular n-contact. Fig. 4(c) displays the ratio (Γ) between the J-V characteristics for the two LEDs where J is calculated in four different ways: i) by using the whole area of the n-contact, and ii, iii, iv) for an annulus area with respectively L_h = 100 μm, 20 μm, and 5 μm. At 12 V, Γ is equal to 2.48 when J is calculated considering method i), while it decreases with smaller annulus areas (1.58 with L_h = 100 μm, 1.06 with L_h = 20 μm, 1.00 with L_h = 5 μm). It is worthwhile to point out that the characteristics of the two LEDs can be compared only for voltages higher than the turn-on value; at lower voltages the quality of the material can alter the behaviour of the characteristics due to the Schokley-Read-Hall recombination process. Also, at low injection regime, the ratio Γ is heavily affected by electrical noise.

Finally, Fig. 4(d) shows the J-V characteristics obtained for an annulus area with L_h = 5 μm. The two curves are overlapped, meaning that the effective hole current spreading length is given by L_h plus the distance between n- and p- contacts, that is 25 μm. It is worth to highlight that no values of L_h are ever reported in literature for ZnO/p-GaN heterostructure LEDs. Instead, for GaN homojunctions LEDs (where L_h data are reported), L_h is about one order of magnitude more than the value calculated in this work [30], [35]. Clearly, the calculated value of L_h mainly depends on the inverted structure (n-p, instead of p-n) and then on the electrical properties of the p-GaN layer, namely the doping level, the mobility, and the hole density. Both a highly-doped layer and a good crystalline quality for p-GaN are recommended to increase the value of L_h. Nevertheless, L_h also depends on other parameters, such as contact resistance, interface defects, and even ZnO crystal quality.

Apart from the influence of the latter secondary parameters, these considerations prove that: i) the n-p contact interspace is a very critical variable in heterojunction ZnO/GaN LED design, and ii) the device layout proposed here, typical for homojunction GaN-based LEDs, does not allow to fabricate large-size LEDs due to the limited hole current spreading length.

Current spreading is not critical in GaN-based homojunction LEDs, since the underlying layer consists of n-GaN which has a large conductivity. In ZnO/GaN-based heterojunction LEDs it is evident that a circular geometry could not be the best way to design the metal electrodes layout and other solutions should be considered.

D. Interdigitated electrodes

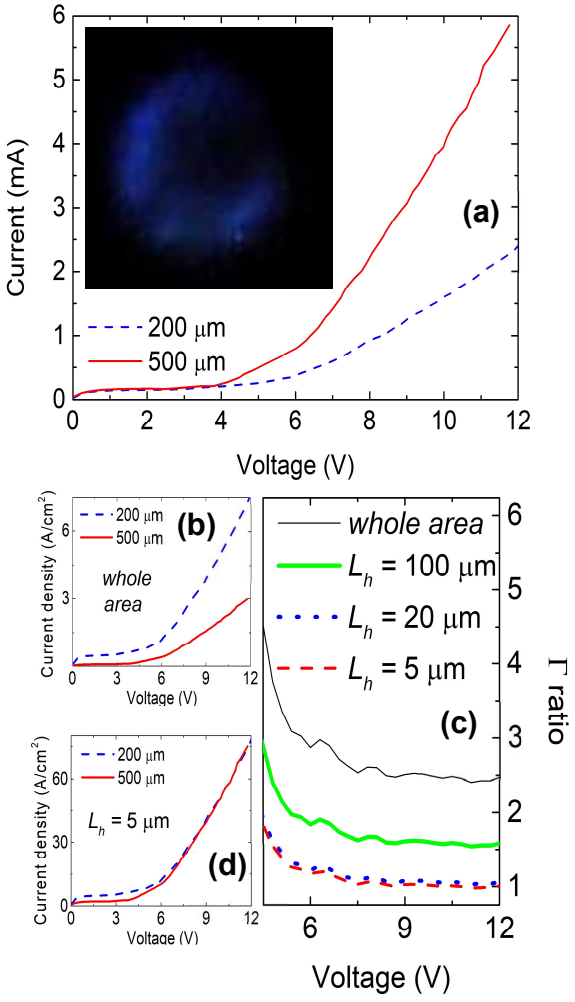

Fig. 4. (a) I-V characteristics for 200 μm- and 500 μm-LEDs with a n-p contact interspace of 20 μm; the inset shows an image of the non-uniform emission coming from the backside of a 200 μm-LED biased at 6.5 V; (b) J-V characteristics of the same LEDs reported in (a) (current is divided by the whole n-contact area); (c) Γ-V curves of the same LEDs reported in (a), calculated considering the whole area of the n-contacts and three different annulus areas; (d) J-V characteristics where current density is obtained by dividing the current by an annulus area with L_h = 5 μm.

A design rule to improve the carrier transport and the injection efficiency of ZnO/GaN LEDs could make use of an interdigitated contact layout instead of the circular one. The adoption of such a structure for emitting devices has been already proposed by Guo *et al.*[36] for GaN-based devices but this is the first time that an interdigitated contact layout is proposed as an alternative to standard circular LED in ZnO/GaN heterostructure LEDs. Having determined that for our samples the hole current spreading length is 25 μm, the width of the fingers was fixed at 15 or 20 μm which is considered to be sufficiently small to allow the holes injected

by the *p*-contact to spread under the whole *n*-contact. The distance between *n* and *p* fingers was either 5 or 20 µm. The length and the number of the fingers were designed to have the same area of circular LEDs fabricated on the same substrate and used for comparison.

Fig. 5 shows the *I-V* characteristics of several both circular and interdigitated LEDs. In order to identify the different LEDs, the notation used is $X_{a,b}$, where "X" is designated as "C" for "circular" or "I" for "interdigitated", and the subscript "a, b" indicates respectively the diameter of the circular LEDs (or the interdigitated version with the same area) and the distance between *n* and *p* electrodes. The two insets in Fig. 5 help one to compare the extent of the circular and the interdigitated LED

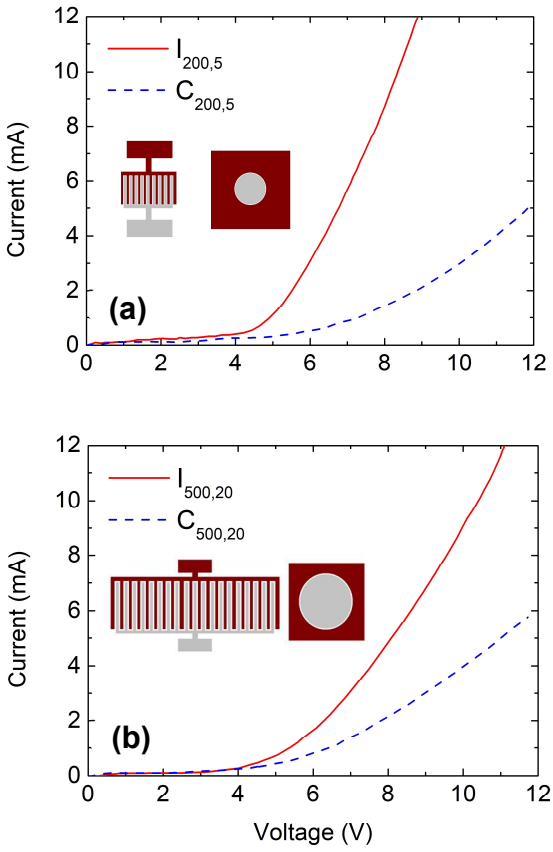

Fig. 5. *I-V* characteristics of (a) 200 µm-circular LED (C) and interdigitated LED (I) of 15 µm-width (having the same area of the 200 µm-circular one) with contact distance d = 5 µm; (b) 500 µm-circular LED µm and interdigitated LED of 20 µm-width (having the same area of the 500 µm-circular one) with contact distance d = 20 µm. The insets show a sketch of the corresponding interdigitated and circular LEDs.

structures. The interdigitated LED $I_{200,5}$ compared to the 200 µm-circular one ($C_{200,5}$), has 9 fingers, each one 200 µm long and 15 µm wide (base of the fingers: 295 µm long and 15 µm wide), corresponding to an emitting area of 31 425 µm^2; the second interdigitated structure $I_{500,20}$ compared to 500 µm-circular one ($C_{500,20}$), has 19 fingers, each one 445 µm long and 20 µm wide (base of the fingers: 1380 µm long and 20 µm wide), corresponding to an emitting area of 196 700 µm^2.

In the interdigitated device the holes are uniformly injected in the *n*-region and the current crowding at the borders is less significant. In this way, the injection turns out to be more efficient and light emission more uniform with respect to the circular design. At 10 V the interdigitated device exhibits an increase of the current by a factor 5 compared to the equivalent circular LED of 200 µm-diameter and a factor 2.25 compared to the 500-µm-diameter LED. On the other hand, the benefits of finger-shaped layout are reduced with the increase of the contact area. In other words, to keep the finger width to a small value (15 or 20 µm in our case), an increase of the emissive surface requires an increase of the length and/or the number of the fingers; consequently, the access surface for the carriers to be injected is noticeably augmented and the current crowding is distributed along the entire perimeter of the electrode. For this reason, at a fixed voltage the interdigitated devices with larger electrode surfaces (500 µm) exhibit a smaller increase of the current.

IV. Conclusions

This work discusses on the carrier injection features in *nid*-ZnO/*p*-GaN heterojunction LEDs with special attention to the structure layout and shows its effects on electrical and optical characteristics. Since in such LEDs the buried layer is the *p*-GaN, carrier transport in the *p* layer is hindered by the low mobility of the *p*-GaN. As a consequence, the recombination in the *n* region is limited in correspondence to the edge of the *n* contact and it is strongly dependent on the distance between the *p*- and the *n*-contacts. A method to calculate the spreading length of the current is proposed and discussed. Moreover, it is proved that an interdigitated electrode structure, applied for the first time to *nid*-ZnO/*p*-GaN heterojunction LEDs, can increase the hole injection efficiency in such devices.

References

[1] Y. K. Mishra and R. Adelung, "ZnO tetrapod materials for functional applications," *Materials Today*, vol. 21, no. 6, pp. 631–651, Jul. 2018.

[2] H. Morkoç and Ü. Özgür, *Zinc oxide: fundamentals, materials and device technology*. Weinheim: Wiley-VCH, 2009.

[3] H. Wang *et al.*, "Fabrication and characterization of alternating-current-driven ZnO-based ultraviolet light-emitting diodes," *Electronic Materials Letters*, vol. 11, no. 4, pp. 664–669, Jul. 2015.

[4] J. J. Hassan *et al.*, "Fabrication of ZnO nanorod/p-GaN high-brightness UV LED by microwave-assisted chemical bath deposition with Zn(OH)2–PVA nanocomposites as seed layer," *Optical Materials*, vol. 35, no. 5, pp. 1035–1041, Mar. 2013.

[5] J. J. Dong *et al.*, "Ultraviolet electroluminescence from ordered ZnO nanorod array/p-GaN light emitting diodes," *Applied Physics Letters*, vol. 100, no. 17, p. 171109, Apr. 2012.

[6] D. J. Rogers, F. Hosseini Teherani, A. Yasan, K. Minder, P. Kung, and M. Razeghi, "Electroluminescence at 375nm from a ZnO⁄GaN:Mg⁄c-Al2O3 heterojunction light emitting diode," *Applied Physics Letters*, vol. 88, no. 14, p. 141918, Apr. 2006.

[7] R.-M. Ko, S.-J. Wang, C.-Y. Chen, C.-H. Wu, Y.-R. Lin, and H.-M. Lo, "Hydrothermal growth of n-ZnO films on a patterned p-GaN epilayer and its application in heterojunction light-emitting diodes," *Japanese Journal of Applied Physics*, vol. 56, no. 4S, p. 04CH03, Apr. 2017.

[8] S. K. Jha, O. Kutsay, I. Bello, and S. T. Lee, "ZnO nanorod based low turn-on voltage LEDs with wide electroluminescence spectra," *Journal of Luminescence*, vol. 133, pp. 222–225, Jan. 2013.

[9] Ya. I. Alivov, J. E. Van Nostrand, D. C. Look, M. V. Chukichev, and B. M. Ataev, "Observation of 430 nm electroluminescence from ZnO/GaN heterojunction light-emitting diodes," *Applied Physics Letters*, vol. 83, no. 14, pp. 2943–2945, Oct. 2003.

[10] J. R. Sadaf, M. Q. Israr, S. Kishwar, O. Nur, and M. Willander, "Forward- and reverse-biased electroluminescence behavior of chemically fabricated ZnO nanotubes/GaN interface," *Semiconductor Science and Technology*, vol. 26, no. 7, p. 075003, Jul. 2011.

[11] G. C. Park *et al.*, "Hydrothermally Grown In-doped ZnO Nanorods on p-GaN Films for Color-tunable Heterojunction Light-emitting-diodes," *Scientific Reports*, vol. 5, no. 1, Sep. 2015.

[12] F. Caruso *et al.*, "Frequency-Downconversion Stability of PMMA Coatings in Hybrid White Light-Emitting Diodes," *Journal of Electronic Materials*, vol. 45, no. 1, pp. 682–687, Jan. 2016.

[13] M. Mosca *et al.*, "Warm white LED light by frequency down-conversion of mixed yellow and red Lumogen," presented at the SPIE Microtechnologies, Grenoble, France, 2013, p. 87670L.

[14] M. Mosca, R. Macaluso, F. Caruso, V. Lo Muzzo, and C. Calì, "The p-type doping of ZnO: Mirage or reality?," in *Advances in Semiconductor Research: Physics of Nanosystems, Spintronics and Technological Applications*, Nova Science Publishers, Inc., New York: D. Persano Adorno and S. Pokutnyi, 2015, pp. 245–282.

[15] I. Tiginyanu *et al.*, "Self-organized and self-propelled aero-GaN with dual hydrophilic-hydrophobic behaviour," *Nano Energy*, vol. 56, pp. 759–769, Feb. 2019.

[16] S. S. Patil, M. A. Johar, M. A. Hassan, D. R. Patil, and S.-W. Ryu, "Anchoring MWCNTs to 3D honeycomb ZnO/GaN heterostructures to enhancing photoelectrochemical water oxidation," *Applied Catalysis B: Environmental*, vol. 237, pp. 791–801, Dec. 2018.

[17] S.-Y. Nam *et al.*, "n-ZnO/i-InGaN/p-GaN heterostructure for solar cell application: n-ZnO/i-InGaN/p-GaN heterostructure for solar cell application," *Phys. Status Solidi A*, vol. 210, no. 10, pp. 2214–2218, Oct. 2013.

[18] Y. Huang *et al.*, "Enhanced photoresponse of n-ZnO/p-GaN heterojunction ultraviolet photodetector with high-quality CsPbBr3 films grown by pulse laser deposition," *Journal of Alloys and Compounds*, vol. 802, pp. 70–75, Sep. 2019.

[19] X. Feng, Y. Zhang, and Z. Wang, "Theoretical study of piezotronic heterojunction," *Sci. China Technol. Sci.*, vol. 56, no. 11, pp. 2615–2621, Nov. 2013.

[20] Y. Shen *et al.*, "Low-voltage blue light emission from n-ZnO/p-GaN heterojunction formed by RF magnetron sputtering method," *Current Applied Physics*, vol. 14, no. 3, pp. 345–348, Mar. 2014.

[21] Q.-M. Fu *et al.*, "Blue/green electroluminescence from a ZnO nanorods/p-GaN heterojunction light emitting diode under different reverse bias," *Applied Surface Science*, vol. 293, pp. 225–228, Feb. 2014.

[22] H.-C. Chen *et al.*, "UV Electroluminescence and Structure of n-ZnO/p-GaN Heterojunction LEDs Grown by Atomic Layer Deposition," *IEEE Journal of Quantum Electronics*, vol. 46, no. 2, pp. 265–271, Feb. 2010.

[23] M. Mosca *et al.*, "Optical, structural, and morphological characterisation of epitaxial ZnO films grown by pulsed-laser deposition," *Thin Solid Films*, vol. 539, pp. 55–59, Jul. 2013.

[24] J. Dai *et al.*, "Atmospheric pressure MOCVD growth of high-quality ZnO films on GaN/Al2O3 templates," *Journal of Crystal Growth*, vol. 283, no. 1–2, pp. 93–99, Sep. 2005.

[25] M. Mosca *et al.*, "Chemical Bath Deposition as a Simple Way to Grow Isolated and Coalesced ZnO Nanorods for Light-Emitting Diodes Fabrication," in *2018 IEEE 4th International Forum on Research and Technology for Society and Industry (RTSI)*, Palermo, 2018, pp. 1–6.

[26] F. Caruso, M. Mosca, R. Macaluso, C. Cali, and E. Feltin, "Well-aligned hydrothermally synthesized zinc oxide nanorods on p-gan without a seed layer," in *2015 IEEE 15th International Conference on Nanotechnology (IEEE-NANO)*, Rome, 2015, pp. 1012–1014.

[27] M. Willander *et al.*, "Intrinsic white-light emission from zinc oxide nanorods heterojunctions on large-area substrates," presented at the SPIE OPTO, San Francisco, California, 2011, p. 79400A.

[28] J.-H. Wu, S.-Y. Liu, S. Li, Y. Jiang, G.-P. Ru, and X.-P. Qu, "The influence of ZnO seed layers on n-ZnO nanostructure/p-GaN LEDs," *Applied Physics A*, vol. 109, no. 2, pp. 489–495, Nov. 2012.

[29] X. Guo and E. F. Schubert, "Current crowding in GaN/InGaN light emitting diodes on insulating substrates," *J. Appl. Phys.*, vol. 90, no. 8, pp. 4191–4195, 2001.

[30] X. Guo and E. F. Schubert, "Current crowding and optical saturation effects in GaInN/GaN light-emitting diodes grown on insulating substrates," *Applied Physics Letters*, vol. 78, no. 21, pp. 3337–3339, 2001.

[31] C. G. Van de Walle, "Hydrogen as a Cause of Doping in Zinc Oxide," *Physical Review Letters*, vol. 85, no. 5, pp. 1012–1015, Jul. 2000.

[32] E. G. Barbagiovanni, V. Strano, G. Franzò, I. Crupi, and S. Mirabella, "Photoluminescence transient study of surface defects in ZnO nanorods grown by chemical bath deposition," *Appl. Phys. Lett.*, vol. 106, no. 9, p. 093108, Mar. 2015.

[33] W. Jing *et al.*, "Effects of the geometries of micro-scale substrates on the surface morphologies of ZnO nanorod-based hierarchical structures," *Applied Surface Science*, vol. 355, pp. 403–410, Nov. 2015.

[34] M. Guo, P. Diao, and S. Cai, "Hydrothermal growth of well-aligned ZnO nanorod arrays: Dependence of morphology and alignment ordering upon preparing conditions," *Journal of Solid State Chemistry*, vol. 178, no. 6, pp. 1864–1873, Jun. 2005.

[35] H. Kim *et al.*, "Consideration of the Actual Current-Spreading Length of GaN-Based Light-Emitting Diodes for High-Efficiency Design," *IEEE J. Quantum Electron.*, vol. 43, no. 8, pp. 625–632, Aug. 2007.

[36] X. Guo, Y.-L. Li, and E. F. Schubert, "Efficiency of GaN/InGaN light-emitting diodes with interdigitated mesa geometry," *Applied Physics Letters*, vol. 79, no. 13, pp. 1936–1938, Sep. 2001.